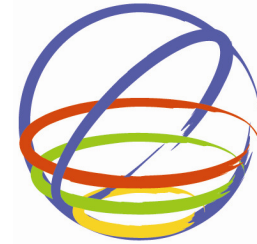


A comparison between existing tsunami load guidance and large-scale experiments with long-waves.

T.O. Lloyd & T. Rossetto

University College London, UK



15 WCEE
LISBOA 2012

SUMMARY:

Design guidance for consideration of tsunami loading on structures has been established by several institutions throughout the world. Much of the research behind these guidelines has been based on the physical modelling of waves generated by traditional paddle generators, capable only of producing short-waves. Short-waves are not necessarily physically representative of tsunami, and research has so far been limited to a few facilities worldwide. A long-wave generator capable of testing at large-scale has been developed in collaboration between UCL and HR Wallingford, in part to address this shortcoming.

This paper presents a review of tsunami research and guidance to date and uses data from experiments carried out using a pneumatic long-wave generator to compare and contrast with design equations in literature. The longer wavelengths generated by our test facility will extend the existing research, providing a more representative platform for improved tsunami design guidance in the future.

Keywords: Tsunami loading, Long-wave generator, Large-scale experiments, Design guidance.

1. INTRODUCTION

Tsunami are water waves caused by earthquakes, volcanic eruptions and underwater or aerial landslides. In deep water, tsunami waves have relatively small heights (typically 0.5-2m), but very long wavelengths (they can reach hundreds of kilometres). As these waves enter the shallower waters of coastal regions, their length reduces and their wave height increases dramatically. The resulting waves can cause violent impacts onto shoreline structures, and the long wavelengths may lead to extensive inundation inland. A requirement exists to devise new and improved methods for the evaluation of tsunami risk to infrastructure, and this has spurred research in the field. The relatively low cost of computing power and advances in numerical modelling techniques over recent years has led to numerical simulation becoming a more viable tool and often a focus for researchers and consultants to explore. In spite of this surge in reliance on numerical modelling, there remain serious deficiencies in the accuracy of numerical tsunami models, particularly in the near-shore and inundation regions. Unfortunately more often than not, it is these regions which are of greatest interest to planners and engineers alike, and a clearer understanding of the near-shore and inundation zone is not just desirable, but critical for designing for tsunami resilience.

Experiments relating to the loading of structures from waves are extensive. The work of Morison et al. (1950), Goda (1974) and later Takahashi & Shimozaki (1994) made large contributions to the design equations used in offshore structures and sea walls, respectively. Loading induced by short-period inundating waves on structures has been examined by Camfield (1991), Asakura et al. (2002), Yeh (2007), and Lukkunaprasit, Thanasisathit & Yeh (2009). Much of this literature has led to the development of design guidance; Okada et al. (2006), and FEMA (2008), which are beginning to be used in real world applications.

The production of these design guides is a welcome step and represents a first attempt to deal with the tsunami aspects of structural design and risk management. However, although some verification of these design equations has been conducted (Lukkunaprasit, Ruangrassamee & Thanasisathit, 2009, Asakura et al., 2002, Fujima et al., 2009), the set-ups of these verification experiments remain similar to the laboratory conditions on which the equations were based. Furthermore, all such experiments, even those carried out at large-scale, (Arikawa, 2009) adopt short-period waves that are not representative of tsunami in the field.

Large wave facilities worldwide almost exclusively use the same type of wave generation system, a moving paddle. While this is perfectly adequate for what is often the day to day work of these facilities, i.e. the modelling of storm waves, the generation of longer waves becomes difficult to a point and impossible after that. Tsunami are long waves, which even at modest scale are impossible to represent correctly using current generation techniques.

This problem was identified, and as part of a collaboration between EPICentre researchers at UCL and HR Wallingford, a new pneumatic long wave generator was designed and built (Rossetto et al., 2011, Charvet, 2012). Some results of the initial testing will be discussed in the context of some key tsunami force guidance in existence.

2. TSUNAMI DESIGN GUIDANCE

Despite the surge in interest following the Indian Ocean tsunami of 2004, there remain relatively few coastal design codes that explicitly cater for the design of structures to resist tsunami. The US Army Corps of Engineers (USACE) released a number of coastal publications over the 60's 70's and 80's which were consolidated with the publication of the Shore Protection Manual (SPM) in 1973. The fourth and final edition of this USAEWES (1984) was the result of various updates and was eventually replaced by the current guidelines; the Coastal Engineering Manual (CEM) (USACE, 2002). The CEM expanded on previous guidance and provided mechanisms for the use of modern computational techniques. However, the CEM still did not include detailed assessment of tsunami because the risk was perceived to be sufficiently small, that tsunami could be completely omitted from design.

Camfield (1980) is a thorough review of the state of the art for tsunami engineering at the beginning of the 1980s. In spite of this document having design formulae for force calculation, it is only briefly mentioned as having further information in the CEM. Many of the formulae in Camfield (1980) can still be found in more recent guidance which will be discussed in the following section.

The Federal Emergency Management Agency (FEMA) produces several design guides for natural hazard design. Its Coastal Construction Manual (FEMA, 2000), was first published in 1981, and its current version gives brief guidance for peak tsunami velocities and depth adjustments as part of its coastal flooding sections. FEMA (2000), as part of its more general flooding guide splits the flood loads into components, some of which are discussed in the following sections. Other research particularly from Japan will be discussed in relation to these components, which generally apply throughout the literature (with a few deviations).

2.1. Velocity equations and elevation terms present in design codes

Tsunami velocity is generally a large source of uncertainty due to sparse measurements from post-tsunami surveys, in comparison with water depth based measurements. Several design guides attempt to estimate the velocity of a wave front, and these are all calculated as a function of some depth term. For this reason, the two quantities are intrinsically linked and are discussed here together. Velocity is an important parameter in several of the loading equations as will be seen in the following sections.

Many of the design guidance in existence use the same formula for estimation of tsunami front velocity and this is given by Eqn. 2.1.

$$u = 2\sqrt{gd} \quad (2.1)$$

Equation 2.1 is common to FEMA (2000), Camfield (1980), USACE (1989) and CRATER (2006) amongst others, where g is the acceleration due to gravity and d is a measure of depth. Searching for a derivation of this expression leads us back to Keulegan (1950), who proposed it by analysis and approximation of the classic dam break problem. Keulegan however used the leading thickness of the surge tongue as d , which is not the same quantity as others have since adopted. FEMA (2000) for example use the design still water level, presumably for simplicity and conservatism. CCH (2000) simply uses the numerical value of water depth, as the velocity.

Other variants arise from experimental work, usually of the same form as Eqn. 2.1, but often multiplied by a different coefficient (instead of “2” in Eqn. 2.1). This can be thought of as a scaling of the offshore wave velocity equation, which for shallow water waves is given by a coefficient of 1.0. In reality, the velocity is unsteady and the highest velocities may not occur at the time of the highest water depths. Other factors become important in its determination, like distance from the shore, slope, and roughness of the bathymetry surface and the period of the wave. The maximum water level will often be associated with little or no velocity as the wave begins to recede, so the use of these formulae outside their original purpose, i.e. initial surge inundation, is meaningless. Even then, the peak velocities recorded by experiments can vary wildly.

Increasingly numerical models are relied upon for estimating velocities of inundations. Unfortunately, due to complexities in the inundation zone, assumptions behind shallow water equations being broken (or at the very least stretched) and a shortage of real validation data, the velocity results of these models should always be viewed with scepticism. However, velocity outputs from numerical models are integral to some of the loading parameters given by FEMA (2008).

2.2. Hydrostatic forces

Hydrostatic forces arise from the presence of stationary water. The hydrostatic force can be further split into two cases; a vertical hydrostatic force which is more commonly known as buoyancy, and lateral hydrostatic force.

The buoyancy force acts in an opposite direction to gravity and occurs due to a difference in density caused by enclosed water-tight or slow filling volumes of a structure being submerged. The density difference between air and water is such that effectively the density of air is zero, and so the buoyancy can be calculated by Eqn. 2.2.

$$F_b = \rho g V \quad (2.2)$$

Where ρ is the density of water, and V is the volume of water displaced by the structure. Eqn. 2.2. is found in FEMA (2000), Camfield (1980), FEMA (2008), amongst other literature.

Lateral hydrostatic forces arise from the variation in pressure distribution with depth. This is a linear function with depth, and takes the form of Eqn. 2.3.

$$p = \rho g d \quad (2.3)$$

By integration, the hydrostatic force on a wall width B , with a dry interior side is given by Eqn. 2.4.

$$F_{hs} = \frac{1}{2} B \rho g d^2 \quad (2.4)$$

This is the basic form of equation used by FEMA and most US based design guides. CCH (2000) use a slightly modified form which instead of d , increases the water depth with a velocity head term, $d + u^2/2g$. This is clearly a slightly more conservative form and increases the hydrostatic force for flowing water. It is also present in PIANC (2010), USNRC (2009) and IMPW (2009).

2.3. Hydrodynamic forces

Greater differences in the treatment of hydrodynamic forces by existing guidance are found than with hydrostatic forces. FEMA guidance takes a change in direction from FEMA (2000), to FEMA (2008). In the earlier document, hydrodynamic force is treated in the same manner as the vast majority of literature and takes the form of a classic drag equation. The pressure is assumed to be proportional to the square of the velocity, u , and to act on the entire exposed surface uniformly with depth. By integration of this pressure, the hydrodynamic force is given by Eqn. 2.5, where C_d is the drag coefficient.

$$F_{hd} = \frac{1}{2} C_d \rho B d u^2 \quad (2.5)$$

This is the same form as seen in Ohmori et al. (2000) as well as most other codes. Yeh (2007) took the equation further and stated that the maximum velocity and maximum water level do not necessarily occur at the same instance. Instead they defined the parameter “momentum flux”, $(du^2)_{\max}$, as the most important for deriving design hydrodynamic forces.

$$F_{hd} = \frac{1}{2} C_d \rho B (du^2)_{\max} \quad (2.6)$$

FEMA (2008) take this concept and use it in their guidance aimed at the design of vertical evacuation structures.

2.4. Impulsive forces

Impulsive forces relate to the initial overshoot associated with the impact of the leading tongue of a wave or surge. There are some differences and some confusion in existing guidance caused by the use of inconsistent definitions. Cross (1967) defines the “surge force” as a combination of the hydrostatic component and an additional dynamic component dependant upon the velocity of the incoming surge and the angle of the surge front. Camfield (1980) use the slope and the Chezy roughness coefficient to estimate the dynamic component as well and then use Eqn. 2.1 to derive a total surge force. The solution contains several approximations, includes the hydrostatic component and results in Eqn. 2.7.

$$F_{imp} = 4.5 B \rho g d^2 \quad (2.7)$$

This is essentially 9 times the hydrostatic force given by Eqn. 2.4.

Ohmori et al. (2000), who was highly influential in the development of the Japanese guidelines of Okada et al. (2006), use the wave angle as a parameter to determine the dynamic component of the surge force. Asakura et al. (2002) demonstrate Eqn. 2.7 by a slightly different derivation from their experimental results (by assuming maxima of his experimental parameters). FEMA (2008) on the other hand, reference the work of Ramsden (1993), which indicated that the maximum overshoot in force from a bore was approximately 1.5 times the hydrodynamic force, F_{hd} . The advised design equation in FEMA (2008) is simply 1.5 times Eqn. 2.6.

Ohmori et al. (2000) also define the impulsive component in terms of the hydrodynamic force. They effectively use the angle of the wave front to modify the drag coefficient in Eqn. 2.5. Assuming, as advised by many codes, a value of C_d of 2 has the effect of making the impulsive component

according to Ohmori et al. (2000) vary from 1 times F_{hd} for a wave angle of 30 degrees, to 1.8 F_{hd} for a slope angle of 45 degrees. The relationship quickly increases for angles larger than this, and its application may not be suitable, without further research.

3. EXPERIMENTAL WORK USING A LONG WAVE GENERATOR

Section 2.0 describes several frameworks which exist to compare design forces on structures with those of real experiments. As a first pass, the data from a short-elevated wave will be examined. The diagnostics from this is then applied to a longer wave in order to ascertain any differences or indeed similarities between the expected forces according to design guidance, and the observed. The set up is described in detail by Rossetto et al. (2011), Lloyd (2012) and Charvet (2012), but briefly is outlined in Fig. 3.1.

The set up shows the operation of the new long wave generator at HR Wallingford. The waves analysed in this paper are elevated waves, but the setup is also capable of generating stable trough led waves.

Fig. 3.1 shows the mechanism behind the generator. Water is vertically displaced in the tank, and released into the flume by varying the tank's internal pressure. This is accomplished by a constant air suction provided by a pump and a computer controlled valve to regulate the pressure. The key benefits of this system over traditional paddle generators are that longer waves can be produced, as well as negative (trough) led waves. Pressures are measured on the building front and side using a series of transducers. Velocities are captured using miniature propeller-meters and the water surface elevation is recorded using a high speed camera pointed through a viewing window at the location of the test specimen. Image processing and computer vision techniques were used to accurately extract the time-dependant elevation profile from the resulting series of still images. This is fully reported in Lloyd (2012).

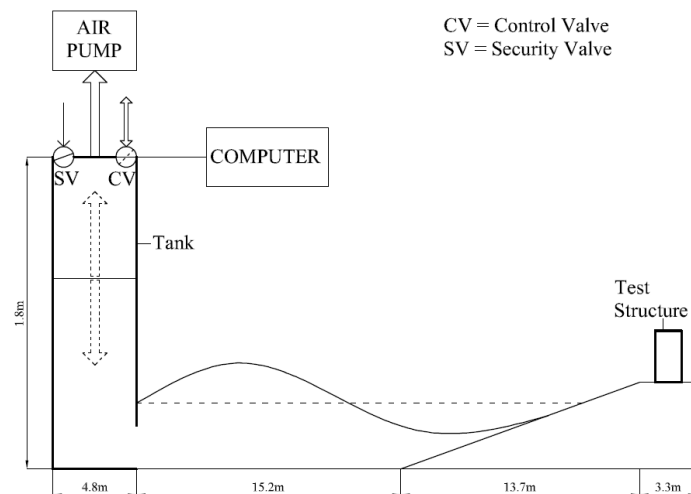


Figure 3.1. Schematic of flume setup at HR Wallingford (not to scale).

The purpose of these experiments was to extend existing knowledge of wave interactions with structures to longer period/wavelength waves than have previously been tested. At the limits of their capabilities, existing generators in other facilities worldwide can generate waves with a maximum period of the order 10s. The new facility can push this limit far further than this and some of our test waves had periods of two minutes. Initially, the lower end of the facility's capability is examined here to provide a base comparison with existing literature.

3.1 Analysis of a long-period wave impact

The shorter wave periods that were generated during our testing at HR Wallingford were of the order of five to ten seconds. Wavelengths of 10 to 20 metres with the relatively shallow water depths we had in our flume, still made our waves technically shallow water waves, and therefore long-period waves.

The “shorter” waves generally exhibited different interaction behaviour than the longer period waves, with the latter more closely resembling flood waves. One of our larger “short” waves has been analysed using the output of image processing, and pressure transducers mounted on the front and side faces of the test structure obstructing the flow. The water elevation at the position of the lower pressure transducer in our array is shown as the red line in Fig. 3.2. The black markers indicate the pressure divided by density times the acceleration due to gravity, g . The resulting pressure indicator has the units of mm of water making it comparable with the red line of the water height.

The interactions with the shorter waves tend to be more energetic creating highly turbulent flow regimes associated with the initial impact. Splashing accounts for some of the initial peak shown in the water elevation profile and at least some unknown quantity of air entrainment is certainly present. This means that the water surface profile around the one second region of Fig. 3.2, does not represent the entire phenomena. Additionally, the initial impact region of the pressure transducer data is highly variable between tests, as is described by Peregrine (1967). The exact nature of this initial impact is still under research, and appears to decrease in significance with increasing wave period. Following the initial peak, there is a transitional part to the profile where air entrainment could account for some of the fluctuations in pressure. After this, the flow settles into a quasi-steady regime. However, one further feature of Fig.3.2 is very clear - that the principle component of the pressure measured by the transducer can be accounted for by hydrostatic pressure alone. Fig. 3.2 effectively represents a comparison between the hydrostatic force equation present in guidelines such as FEMA (2008) (Eqn. 2.4) and the pressures recorded in our tests.

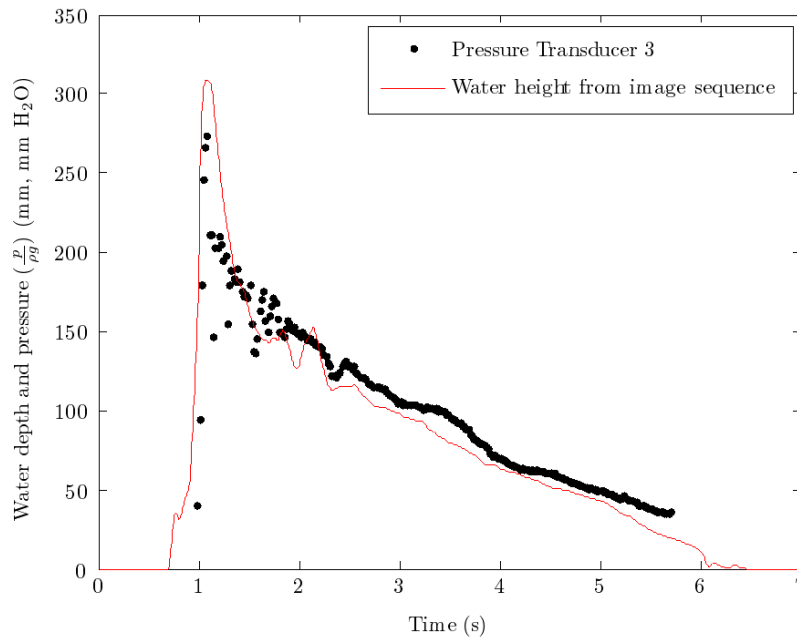


Figure 3.2. Comparison between water surface elevation and hydrostatic pressure derived depth.

In order to draw comparisons to the other formulae present in design guidance, the velocity must also be examined in conjunction with the quantities in Fig. 3.2. The velocity immediately in front of the structure was used for this purpose for the remainder of the paper, though the full velocity field will be used for future work.

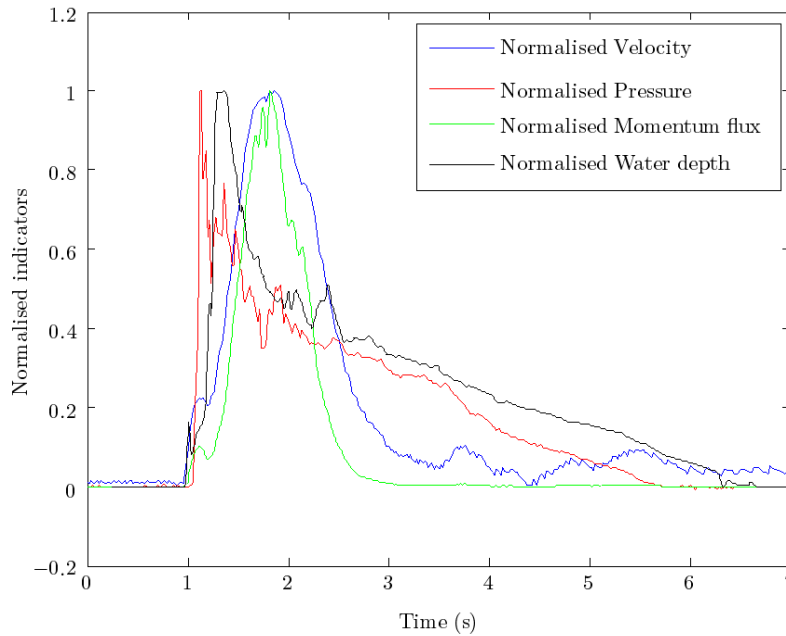


Figure 3.3. Normalised indicator parameters showing their relative contributions with time.

Using this additional information a picture can be drawn of the relevant force indicators as specified by the various guidance literature. Namely; water depth, velocity and momentum flux. The three quantities are normalised by their maxima for our example, and displayed in Fig. 3.3. This plot illustrates the importance of time-dependence in the calculation of force components. A limitation of design formulae in existing guidance is that they often only indicate maxima and the time evolution of the loads is neglected. This is usually conservatively dealt with by using high factors of safety and appropriate load cases as in FEMA (2008). However, the design equations in the range of guidance described in section two are all entirely based on short period wave experiments. This time dependency requires a more in-depth analysis to check that the guidance equations are indeed conservative, and whether any other physical processes occur and are important as the wavelength is increased.

The next step in comparing the contributions of these indicators is to use them to derive the two principle components of force, hydrostatic, and hydrodynamic. The blue and red lines in Fig. 3.4 are the hydrostatic and hydrodynamic components of force based on FEMA (2008) (and most others). These values were derived from the velocity and image based water depth data and combined. The “total force” using these two components is given by the thick green line. The thick black line indicates the total integrated force as measured by the pressure transducers on the front and side faces. These point pressures were interpolated to produce a surface pressure distribution over a 1mm grid. The interpolated pressures multiplied by their 1mm² areas were then added together to integrate the pressure numerically giving an indication of the total force on the structure. This method cannot capture shear stress on the side surface, but as the test structure is effectively a bluff body, shear stresses are minimal in comparison to normal stresses and can be largely ignored (Massey, 1970).

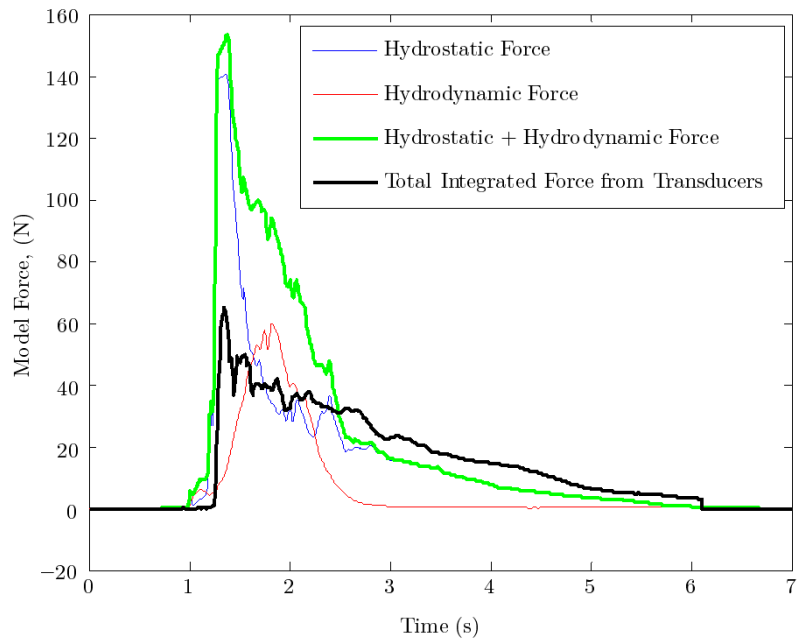


Figure 3.4. Major components of force as given by design guidance, plotted against measured total force.

The green line in Fig. 3.4 represents the combined hydrostatic and hydrodynamic force as given by Eqn. 2.4 and 2.6 respectively from FEMA (2008). Although it should be noted, the design equations deal with maxima, rather than time-varying loading as shown here, a notable disparity can be seen between the integrated-pressure (force) readings on our structure (black) and the predicted forces from various guidance documents. The initial peak should be ignored in this case, as the high predicted hydrostatic force is based on a potentially unreliable water elevation measurement and high air-entrainment due to splashing. The level recorded at the front of the structure is a relatively thin layer associated with the splash up of the impact water.

This meant that the vertical pressure distribution was not linear at the time of impact and the density was also affected by the presence of large volumes of air in the fluid. After this initial impact, the hydrostatic force drops down to approximately the measured level of the transducers, whereas the hydrodynamic component causes the combined force to remain higher than our measured force indicates. After 2.5 seconds, a drop off in velocity means the hydrodynamic component of the design equations becomes insignificant, and this causes the design equations to under-predict the total force measured by our pressure transducers. This difference is under investigation, but could be due to added mass forces produced by the deceleration of the flow past our obstruction. This occurs during the quasi-steady phase of the interaction and will be fully investigated using additional steady-state tests planned over the summer 2012. Further confirmation or rejection of this hypothesis will be presented in the oral presentation.

4. CONCLUSIONS

One wave has been analysed and presented in this paper. The wave was one of the shorter tests of our possible waves for selection, and chosen because it is more comparable with the tests originally used by others to derive current design guidance. Longer-period waves are still under investigation and will be examined in detail during the oral presentation. The sample short-wave has shown the relative contributions of the hydrostatic and hydrodynamic components as well as a potential added-mass component rarely mentioned in guidance.

Full analysis of the time-dependant nature of waves has been demonstrated to be important in Fig. 3.3,

whereas current design guides generally only generally consider maxima. The extension of our wavelength generation capabilities will determine whether the current design equations are sufficient, whether they require additional refinement, or whether an entirely new approach would be preferable. The approach of Yeh (2007) appears to rightly identify that the peak velocity and peak velocity do not necessarily occur at the same instance, and this is reflected in their use of (maximum) momentum flux to determine the hydrodynamic component. However, our initial findings indicate that hydrostatic rather than hydrodynamic forces appear to be the dominant component; in which case the time-dependency may not be important for these loads. In any case, the further investigation of this effect is essential.

Based on the outcome of this initial test, the (maxima-based) equations given in section two would appear to be conservative. However, the further investigation of longer period waves may indicate otherwise, and certainly noticeably produce different flow regimes. The flow regimes of the longer period waves are closer to the quasi-steady flows characterised by the tail-end of Fig.3.4, where our measured forces exceed those predicted by design guidance. This produces an obvious cause for concern and makes further analysis of the other longer period waves in our sample of utmost importance.

ACKNOWLEDGEMENT

This research has been funded by an EPSRC Industrial CASE studentship and Arup, who are the industrial partner. The authors thank HR Wallingford for their technical support with the experiments. William Allsop (HWR), Ziggy Lubkowski (Arup), Ian Eames (UCL), Ingrid Charvet (UCL) and Tristan Robinson (UCL) are all personally thanked for their contributions to the experiments and data interpretation.

REFERENCES

- Arikawa, T. (2009). Structural Behavior Under Impulsive Tsunami Loading, *Journal of Disaster Research* **4:6** 377–381.
- Asakura, R., Iwase, K., Ikeya, T., Takao, M., Kaneto, T., Fujii, N. & Ohmori, M. (2002). The tsunami wave force acting on land structures, *Proceedings of Coastal Engineering 2002*, **1**, 1191–1202.
- Camfield, F. E. (1980). *Tsunami Engineering*. Special Report No. 6, US Army Coastal Engineering Research Center, Fort Belvoir, Virginia.
- Camfield, F. E. (1991). Wave Forces on Wall, *Journal of Waterway, Port, Coastal and Ocean Engineering* **117:1**, 76–79.
- CCH (2000). City and County of Honolulu Building Code (CCH), Tech. Standard. Chapter 16, Article 11: Regulations Within Flood Hazard Districts and Developments Adjacent to Drainage Facilities, Department of Planning and Permitting of Honolulu, Hawaii, Honolulu, HI.
<http://www1.honolulu.gov/council/ocs/roh/16a11.pdf>
- Charvet, I. (2012). Experimental modelling of long elevated and depressed waves using a new pneumatic wave generator, PhD thesis, University College London, UK.
- CRATER (2006). Reduce Tsunami Risk - strategies for urban planning and guidelines for construction design, CRATER, Coastal Risk Analysis of Tsunamis and Environmental Remediation - The Italian Ministry for the Environment, Land and Sea & the Asian Disaster Preparedness Centre, Bangkok.
- Cross, R. H. (1967). Tsunami surge forces, *Journal of the waterways and harbors division* **93:4**, 201–231.
- FEMA (2000). *Coastal Construction Manual*, third edition FEMA 55, Federal Emergency Management Agency, Washington D.C.
- FEMA (2008). *Guidelines for Design of Structures for Vertical Evacuation from Tsunamis*, Technical Report P646, Federal Emergency Management Agency, Washington D.C.
- Fujima, K., Achmad, F., Shigihara, Y. & Mizutani, N. (2009). Estimation of Tsunami Force Acting on Rectangular Structures, *Journal of Disaster Research* **4:6**, 404–409.
- Goda, Y. (1974). New wave pressure formulae for composite breakwaters, *Proceedings of the 14th International Coastal Engineering Conference*, **3**, 1702–1720.
- IMPW (2009). *Guidelines for Planning of Infrastructure and General Development in Regions Prone to Tsunami*, (in Indonesian). No. 06/PRT/M/2009, Indonesian Ministry of Public Works (IMPW), Jakarta.
- Keulegan, G. (1950). Wave motion, in Hunter Rouse (ed.), *Engineering Hydraulics*, *Proceedings of the Fourth Hydraulics Conference*, John Wiley & Sons, Inc, New York, pp. 711–768.
- Lloyd, T. O. (2012). MPhil Transfer Report. Vulnerability of coastal infrastructure to tsunami: Analytical and

- experimental study., Master's thesis, Department of Civil Environmental and Geomatic Engineering, University College London.
- Lukkunaprasit, P., Ruangrassamee, A. & Thanasisathit, N. (2009). Tsunami loading on buildings with openings, *Science of Tsunami Hazards* **28:5**, 303–310.
- Lukkunaprasit, P., Thanasisathit, N. & Yeh, H. H. (2009). Experimental Verification of FEMA P646 Tsunami Loading, *Journal of Disaster Research* 4:6, 410-418
- Massey, B. (1970). *Mechanics of fluids*, Van Nostrand Reinhold Company Ltd.
- Morison, J., O'Brien, M., Johnson, J. & Schaaf, S. (1950). The Force Exerted by Surface Waves on Piles, *Petroleum Transactions* **189**, 149–154.
- Ohmori, M., Fujii, N. & Kyotani, O. (2000). The numerical computation of the water level, the flow velocity and the wave force of the tsunami which overflow the perpendicular revetments - (in Japanese), *Proceedings of the Coastal Engineerings of JSCE* **47**, 376–380.
- Okada, T., Ishikawa, T., Tateno, T., Sugano, T. & Takai, S. (2006). Tsunami loads and structural design of tsunami refuge buildings, Technical report, The Building Centre of Japan.
- Peregrine, D. H. (1967). Long waves on a beach, *Journal of Fluid Mechanics* **27:4**, 815–827.
http://www.journals.cambridge.org/abstract_S0022112067002605
- PIANC (2010). Mitigation of tsunami disasters in ports, PIANC Report 112, PIANC, Bruxelles.
- Ramsden, J. D. (1993). Tsunamis : Forces On A Vertical Wall Caused By Long Waves, Bores, And Surges On A Dry Bed, PhD Thesis, California Institute of Technology.
- Rossetto, T., Allsop, W., Charvet, I. & Robinson, D. I. (2011). Physical modelling of tsunami using a new pneumatic wave generator, *Coastal Engineering* **58:6**, 517–527.
<http://linkinghub.elsevier.com/retrieve/pii/S0378383911000135>
- Takahashi, S. & Shimosako, K. (1994). Wave pressure on a perforated wall, *Proc., Int. Conf. on Hydro-Technical Engineering for Port and Harbor*, Japan.
- USACE (1989). Water Levels and Wave Heights for Coastal Engineering Design, Engineer Manual EM 1110-2-1414, U.S. Army Corps of Engineers, Washington D.C.
- USACE (2002). Coastal Engineering Manual (CEM), Engineer Manual EM 1110-2-1100, U.S. Army Corps of Engineers, Washington D.C.
- USAEWES (1984). Shore Protection Manual, (SPM) 4th ed., 2 Vol, U.S. Army Engineer Waterways Experiment Station, U.S. Government Printing Office, Washington D C.
- USNRC (2009). Tsunami hazard assessment at nuclear power plant sites in the united states of america, Technical Report NUREG/CR-6966, United States Nuclear Regulatory Commission, USA.
- Yeh, H. H. (2007). Design Tsunami Forces for Onshore Structures, *Journal of Disaster Research* **2:6**, 531–536.